Waveform-Agile Tracking In Heavy Sea Clutter

Sandeep P. Sira, Antonia Papandreou-Suppappola, Darryl Morrell†, and Douglas Cochran
SenSIP Center, Department of Electrical Engineering, Arizona State University, Tempe, AZ 85282, USA
†Department of Engineering, Arizona State University at the Polytechnic Campus, Mesa, AZ 85212, USA
Email: {ssira, papandreou, morrell, cochran}@asu.edu

***Abstract*— The detection and tracking of small targets on the ocean surface is a challenging problem due to low signal-to-clutter ratio (SCR) that results from low grazing angles and high sea state. Recent advances in sensing technologies have enabled waveform-agile schemes that tailor the sensor waveform to match the overall sensing objective. In this paper, we propose a methodology to dynamically adapt the transmitted waveform to improve the tracking performance for scenarios characterized by heavy sea clutter. Employing the compound-Gaussian model for sea clutter, we develop an algorithm for online design of a phase-modulated waveform that improves the SCR in a range bin of interest. A particle filter tracker uses the measurements obtained by this waveform to estimate the target state. We present a simulation study to demonstrate that our scheme leads to improved tracking performance.**

I. Introduction

Waveform diversity is fast becoming one of the most important methods by which sensing systems can be dynamically adapted to their environment and task to achieve performance gains over non-adaptive systems. With recent advances in sensor hardware, this adaptation can involve the changing of the transmitted waveform 'on-the-fly' so as to obtain information that optimally contributes to back-end sensing algorithms such as trackers and detectors. The benefits of such adaptation include improved performance and reduced sensor usage leading to greater system efficiency. Waveform-agile sensing has recently received wide attention with a number of investigations for target tracking [1]–[3], detection [4]–[6], and classification [7], [8], reported in the literature.

Most investigations of waveform-agile tracking have focused on the exploitation of the delay and Doppler resolution properties of transmitted waveforms to estimate the range and velocity of a target in accordance with the dynamically changing uncertainty of the tracker [1]–[3], [9]. Here, the impact of a particular waveform on the measurement errors was quantified by the Cramér-Rao lower bound (CRLB), which is derived from the curvature of the waveform ambiguity function at the origin in the delay-Doppler plane [10]. Since this characterization ignores the sidelobes of the ambiguity function, it does not seem appropriate in situations involving low signal-to-noise ratio (SNR) or low SCR.

Furthermore, recent work on dynamic waveform adaptation for target tracking has often assumed perfect detection [1], or simplistic clutter models [3], [9], [11]. While this may be appropriate when the SNR is high, neither assumption is justified in scenarios that involve heavy sea clutter. Early investigations [12] of the design of waveforms for clutter rejection assumed Gaussian models for sea clutter echoes. Such models are now known to be inadequate due to the higher spatial resolution offered by modern radars. As a result, the compound-Gaussian model for sea clutter has gained wide acceptance [13], [14]. Although there has been extensive research in the development of detection strategies for targets in non-Gaussian sea clutter [15], very few applications of dynamic waveform-adaptation to improve target tracking performance in the presence of non-Gaussian interference have been reported to date.

In this paper, we approach the challenging problem of tracking a small target in heavy sea clutter with the premise that improved detection performance also leads to improved tracking performance. This is due to the fact that, for a given probability of detection, a lower probability of false alarm implies less uncertainty in the origin of the measurement which leads to lower tracking error [16]. Using a previously developed procedure for dynamic waveform design for detecting targets in low SCRs [6], we develop a particle filter based tracker that uses the measurements obtained by the adapted waveform. A simulation study based on parameters derived from real sea clutter measurements demonstrates that our approach provides significant reduction in the tracking root mean square error (RMSE) when compared to a non-adaptive system.

The paper is organized as follows. In Section II, we describe the models for the target dynamics, clutter, and observations. Section III discusses the dynamic waveform design algorithm and the estimation of clutter statistics. In Section IV, we present the target tracker in detail, while in Section V, we provide the results of a simulation study.

II. Target, Signal, and Clutter Models

Let $\mathbf{X}_k = [r_k \;\; \dot{r}_k]^T$ define the state of a target at time k, where r_k and $\dot{r}_k$ are the range and radial velocity, respectively, with respect to a fixed radar. We assume a linear dynamics model for the target motion so that

$$\mathbf{X}_k = F\mathbf{X}_{k-1} + \mathbf{W}_k, \tag{1}$$

where $\mathbf{W}_k$ is a zero-mean, white Gaussian noise sequence with covariance matrix Q. The constant matrices F in (1) and Q are given by

$$F = \begin{bmatrix} 1 & \Delta T \\ 0 & 1 \end{bmatrix}, \quad Q = q \begin{bmatrix} \frac{\Delta T^3}{3} & \frac{\Delta T^2}{2} \\ \frac{\Delta T^2}{2} & \Delta T \end{bmatrix},$$

respectively, where ΔT is the interval between two observations and q is a constant.

A. Received Signal Model

We consider a medium pulse repetition frequency (PRF) radar that transmits a burst of $2L$ pulses in each dwell in an area or direction of interest as shown in Fig. 1. Each dwell consists of two sub-dwells, Sub-dwells 1 and 2, during which L *identical* pulses of the waveforms $s_1(t)$ and $s_2(t)$ are transmitted, respectively. At the end of Sub-dwell 2, a measurement is provided to the target tracker. While $s_1(t)$ is a fixed waveform, $s_2(t)$ is dynamically designed to improve the SCR at a predicted target location, thus improving the tracking performance.

With $s(t)$ denoting either $s_1(t)$ or $s_2(t)$, the received signal at the lth pulse, $l = 0, 1, \ldots, L-1$, in each sub-dwell, is

$$\begin{aligned} g^l(t) &= b^l s(t-\tau_0)\exp(j2\pi\nu_0 t) \\ &+ \sum_i x_i^l s(t-\tau_i)\exp(j2\pi\nu_i t) + n(t), \end{aligned} \quad (2)$$

where b^l, τ_0 and ν_0 are the complex reflectivity, delay and Doppler shift, respectively, of the target (if present), x_i^l, τ_i and ν_i are the complex reflectivity, delay and Doppler shift of the ith clutter scatterer, respectively, and $n(t)$ is additive noise. In (2), we have assumed that the delay and Doppler shift of each scatterer remains constant across the duration of the Sub-dwell, which is reasonable if the PRF is high (in the order of 10 kHz). Note that we make no assumption on the values of the target or clutter Doppler shift so that discrimination of the target based on Doppler differences alone is not possible. We will henceforth assume a high clutter-to-noise ratio so that the clutter is the dominant component and additive noise is negligible. Since we only consider transmitted signals of very short duration, the Doppler resolution is very poor. Therefore, we completely ignore Doppler processing and restrict our attention to delay or range estimation alone.

The received signal in (2) is sampled at a rate f_s to yield the sequence $g^l[n] = g^l(n/f_s)$, which upon matched filtering yields the sequence $y^l[n]$. We define

$$\mathbf{y}_j = [y^0[j], \ldots, y^{L-1}[j]]^T$$

as the vector of matched-filter outputs at delay or range bin j, so that

$$\mathbf{y}_j = \mathbf{b} z_s[j-n_0] + \sum_{n=-(N-1)}^{N-1} z_s[n]\,\mathbf{x}_{j+n}, \quad (3)$$

where

$$\begin{aligned} \mathbf{b} &= [b^0, b^1, \ldots, b^{L-1}]^T, \\ \mathbf{x}_i &= [x_i^0, x_i^1, \ldots, x_i^{L-1}]^T, \end{aligned}$$

n_0 is the range bin that contains the target, and $z_s[m] = \sum_{n=0}^{N-1} s[n]s^*[n-m], |m| < N$ is the autocorrelation function of $s[n] = s(n/f_s), n = 0, \ldots, N-1$.

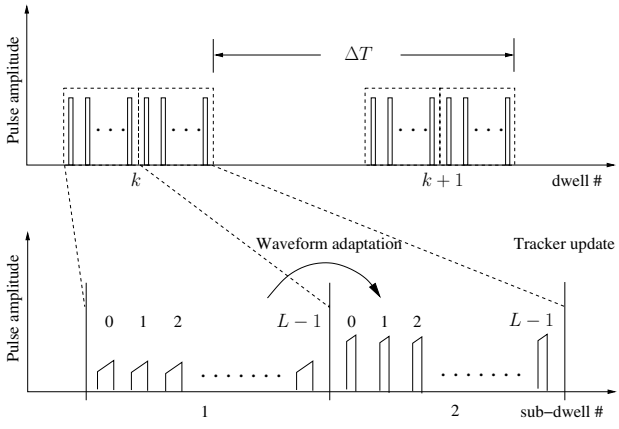

Fig. 1. Pulse diagram of the proposed adaptation algorithm. The pulse amplitudes are for illustrative purposes only.

B. Clutter and Target Models

Early investigations of waveform design for sea clutter rejection typically assumed a Gaussian model for the echoes [12]. As the spatial resolution of radars improved, however, this model could not account for the increased occurrence of higher amplitudes or *spikes*. As a result, a compound-Gaussian model for sea clutter has gained wide acceptance [14] and has received theoretical and empirical support. This model postulates that sea clutter returns are the result of two components: a speckle-like return that arises due to a large number of independent scattering centers reflecting the incident beam, and a texture caused by large-scale swell structures that modulates the local mean power of the speckle return. Given the texture and speckle covariance, the complex reflectivity of the ith clutter scatterer is a circular complex zero-mean Gaussian random vector [15] or $\mathbf{x}_i \sim \mathcal{CN}(0, \mathcal{T}_i\mathbf{\Sigma})$, where $\mathcal{T}_i \geq 0$ is the texture, and $\mathbf{\Sigma} \in \mathbb{C}^{L\times L}$ is the speckle covariance matrix. The speckle remains correlated over a short interval ($\sim$10 ms) while the texture exhibits longer decorrelation time ($\sim$50 s) [17]. Thus at the PRF we consider, $\mathbf{\Sigma} \neq \mathbb{I}_L$ is non-white, where $\mathbb{I}_L$ is the $L\times L$ identity matrix. We will assume that the texture remains constant during a dwell, i.e. over a duration of 2-3 ms. We also assume a Swerling I target [18], so that $\mathbf{b} \sim \mathcal{CN}(0, \sigma^2\mathbb{I}_L)$. From (3) it follows that

$$\mathbf{y}_j \sim \mathcal{CN}(0, \sigma^2\mathbb{I}_K|z_s[j-n_0]|^2 + \mathbf{\Sigma}\beta_j),$$

where the scalar

$$\beta_j = \sum_{n=-(N-1)}^{N-1} \mathcal{T}_{j+n}|z_s[n]|^2$$

is a function of the waveform due to its dependence on $z_s[n]$.

C. Observations Model

At the end of Sub-dwell 2 of the kth dwell, the measurement provided to the tracker is

$$\mathbf{Y}_k = [\mathbf{y}_{\hat{n}_0-n_v}^T, \ldots, \mathbf{y}_{\hat{n}_0}^T, \ldots, \mathbf{y}_{\hat{n}_0+n_v}^T]^T,$$

where $\hat{n}_0$ is the range bin corresponding to the predicted target range, $n_v = (V_k - 1)/2$, where V_k is the number of range bins in the validation gate at time step k [16], while $\mathbf{y}^T$ denotes the transpose of $\mathbf{y}$. Since the observations of target range are quantized to range bins, we will assume that the actual target range is uniformly distributed across the length of the range bin.

III. Dynamic Waveform Design

From (3), we can see that the matched-filter output is a convolution of the radar scene with the autocorrelation function of the transmitted signal. This results in a waveform-dependent smearing of energy from one range bin to another. Clearly, the impact of the 'out-of-bin' clutter is to reduce the SCR in a particular range bin. Our objective is to improve the SCR in Sub-dwell 2 in range bin $\hat{n}_0$, where the target has been predicted. To this end, we seek to design $s_2[n]$ so that its autocorrelation function $z_{s_2}[m]$ is small where the clutter is strong, thus minimizing the effect of out-of-bin clutter in the predicted target location. To achieve this, we first require estimates of the clutter power or texture in the bins whose scatterers contribute to the return $\mathbf{y}_{\hat{n}_0}$.

A. Estimation of Clutter Statistics

Although, the texture is a random process, the assumption that it is practically constant across a dwell permits us to treat its realizations in each range bin as deterministic but unknown variates. Accordingly, suppose that we wish to estimate

$$\Theta = \{\mathcal{T}_{\hat{n}_0-2(N-1)}, \ldots, \mathcal{T}_{\hat{n}_0}, \ldots, \mathcal{T}_{\hat{n}_0+2(N-1)}, \mathbf{\Sigma}\}.$$

From (3), we see that there is a many-to-one linear mapping between the scatterer reflectivities and the matched-filtered output vectors which precludes the exact determination of Θ. Therefore, we instead seek its maximum-likelihood estimate (MLE) that maximizes $p(\mathbf{y}; \Theta)$, where

$$\mathbf{y} = [\mathbf{y}^T_{\hat{n}_0-(N-1)}, \ldots, \mathbf{y}^T_{\hat{n}_0}, \ldots, \mathbf{y}^T_{\hat{n}_0+(N-1)}]^T.$$

To find this MLE however, we must perform a complicated multi-dimensional search since the elements of $\mathbf{y}$ are strongly correlated. Instead, we use the expectation-maximization (EM) [19] algorithm to find $\hat{\Theta}$ that maximizes $p(\mathbf{x}; \Theta)$, where

$$\mathbf{x} = [\mathbf{x}^T_{\hat{n}_0-2(N-1)}, \ldots, \mathbf{x}^T_{\hat{n}_0}, \ldots, \mathbf{x}^T_{\hat{n}_0+2(N-1)}]^T$$

is the *unobserved* or *complete* data vector. Starting with an initial guess $\hat{\Theta}^{(0)}$, the EM algorithm iterates

$$U(\Theta, \hat{\Theta}^{(u)}) = E\{\ln p(\mathbf{x}; \Theta) | \mathbf{y}, \hat{\Theta}^{(u)}\}, \quad (4)$$

$$\hat{\Theta}^{(u+1)} = \arg\max_{\Theta} U(\Theta, \hat{\Theta}^{(u)}), \quad (5)$$

until the change in $\hat{\Theta}$ falls below a set threshold. Note that $\mathbf{x}$ is complex Gaussian distributed and its elements are independent, given the texture and speckle covariance matrix. Together with the fact that $\mathbf{y}$ and $\mathbf{x}$ are related through a linear transformation, this simplifies the computations in (4) and (5).

B. Phase modulated waveform design

After estimation of Θ, as described in Section III-A, let us assume that we have formed the (possibly disconnected) set Z_τ of range bin indices in the $N-1$ neighborhood of $\hat{n}_0$, where the clutter power is large. For example, this could consist of the $N_T < 2(N-1)$ largest values of the estimated texture $[\hat{\mathcal{T}}_{\hat{n}_0-(N-1)}, \ldots, \hat{\mathcal{T}}_{\hat{n}_0+(N-1)}]$ excluding $\hat{\mathcal{T}}_{\hat{n}_0}$ itself, as it corresponds to the predicted target location. In order to minimize the out-of-bin clutter contribution to $\mathbf{y}_{\hat{n}_0}$ in Sub-dwell 2, we seek to minimize $\sum_{Z_\tau} |z_{s_2}[m]|^2$.

To achieve this, we choose a unimodular phase-modulated waveform [20],

$$s_2[n] = \exp(j\lambda_n), n = 0, 1, \ldots, N-1,$$

as a template, and seek to minimize the cost function

$$J(\boldsymbol{\lambda}) = \sum_{Z_\tau} |z_{s_2}[m]|^2, \quad (6)$$

where $\boldsymbol{\lambda} = [\lambda_0, \lambda_1, \ldots, \lambda_{N-1}]^T$. Note that the least squares minimization in (6) is a simplified form of a method that may be used to design a waveform with an arbitrary autocorrelation function. Further, if the minimization is carried out over the time and frequency plane, the same approach can be used to design a waveform with a specified ambiguity function.

It is relatively straightforward to obtain $z_{s_2}[m]$ [3]. The minimization of $J(\boldsymbol{\lambda})$ in (6) can then be easily accomplished using the Newton-Raphson method.

IV. Target Tracking

The target tracker estimates the posterior probability density function $p(\mathbf{X}_k | \mathbf{Y}_{1:k})$ of the target state at dwell k given the observations upto and including dwell k [16]. Although the observation $\mathbf{Y}_k$ provides a measurement of the range of the target, note that it is accompanied by noise that is uniformly distributed across the extent of the range bin. Therefore, despite the fact that the observations model is a linear function of the target state, we cannot use the Kalman filter as the target tracker. Thus, we use the particle filter [21] which estimates the posterior density as a collection of N_p samples or particles $\mathbf{X}^i_k, i = 1, 2, \ldots, N_p$, and their corresponding weights w^i_k. At each dwell, the density is predicted forward in accordance with the target dynamics model and updated according to the likelihood function.

When targets are to be tracked in the presence of clutter, probabilistic data association is often used to counter the uncertainty in the origin of the measurements [16]. In this approach, the likelihood function is usually computed as the average

$$p(\mathbf{Y}_k | \mathbf{X}^i_k) = \sum_m p(\mathbf{Y}_k | \mathbf{X}^i_k, \Omega_m) p(\Omega_m),$$

where Ω_m is an association hypothesis. In our case, however, due to the availability of estimates of the clutter and target statistics in each range bin, we are able to directly compute the likelihood functions $p(\mathbf{Y}_k | \mathbf{X}^i_k)$.

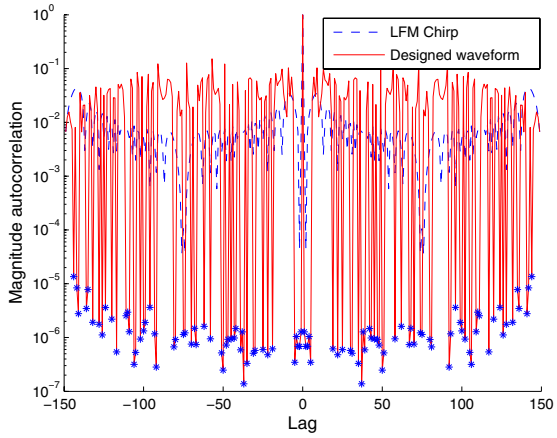

Fig. 2. Magnitude autocorrelation function for a linear frequency modulated (LFM) chirp and the designed phase-modulated waveform. The range bins with strong clutter are marked with asterisks.

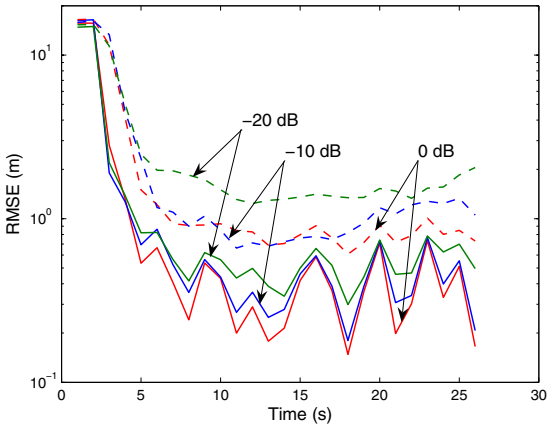

Fig. 3. Comparison of averaged position RMSE at the end of Sub-dwell 1 (dotted lines) and Sub-dwell 2 (solid lines) using the designed waveform. The numbers on the curves indicate SCR in dB.

For this purpose, let n_0^i denote the range bin that contains the range corresponding to $\mathbf{X}_k^i$. With

$$\mathbf{z}_{s_2} = [z_{s_2}[-(N-1)], \ldots, z_{s_2}[0], \ldots, z_{s_2}[N-1]]^T,$$

let

$$\mathbf{H} = \begin{bmatrix} \mathbf{z}_{s_2} & 0 & \ldots & \ldots & 0 \\ 0 & \mathbf{z}_{s_2} & 0 & \ldots & 0 \\ \vdots & \vdots & \vdots & \ddots & \vdots \\ 0 & \ldots & \ldots & 0 & \mathbf{z}_{s_2} \end{bmatrix} \otimes \mathbb{I}_L$$

where $\otimes$ indicates the Kronecker product. Furthermore, let

$$\begin{aligned} \mathbf{T} &= \text{diag}[\hat{\mathcal{T}}_{\hat{n}_0-n_k}, \ldots, \hat{\mathcal{T}}_{\hat{n}_0}, \ldots, \hat{\mathcal{T}}_{\hat{n}_0+n_k}] \otimes \hat{\mathbf{\Sigma}}, \\ \mathbf{V} &= \text{diag}[v_{\hat{n}_0-n_v}, \ldots, v_{\hat{n}_0}, \ldots, v_{\hat{n}_0+n_v}] \otimes \mathbb{I}_L, \end{aligned}$$

where $n_k = n_v + (N-1)$, $v_j = \hat{\sigma}_j^2 \delta[j - n_0^i]$, $\delta[\cdot]$ is the Kronecker delta, and $\hat{\sigma}_j^2$ is the MLE of σ^2, given that the target is in range bin j. The covariance matrix of $\mathbf{Y}_k$, given $\mathbf{X}_k^i$, is then given by

$$\tilde{\mathbf{\Sigma}}_i = \mathbf{H}(\mathbf{T} + \mathbf{V}).$$

From (3), $\mathbf{Y}_k$ is a zero-mean, complex Gaussian vector and hence the weight $w_k^i \propto p(\mathbf{Y}_k|\mathbf{X}_k^i) = \mathcal{CN}(0, \tilde{\mathbf{\Sigma}}_i)$ can be easily computed.

V. Simulations

In our simulation study, a target is tracked as it moves in the presence of simulated heavy sea clutter. At the start of each tracking sequence of 25 dwells, the target is located at a distance of 10 km from the sensor and moves away from it at a near constant velocity of 5 m/s. The clutter scatterers are distributed uniformly in range across the range cells, and uniformly in Doppler over [-1,000, 1,000] Hz. The clutter reflectivity is sampled from a K-distribution with the necessary speckle and texture temporal correlations derived from real sea clutter data as in [3], [17]. The particles at the start of each tracking sequence are drawn from $p(\mathbf{X}_0) = \mathcal{CN}(\mathbf{X}_0, P_0)$, where $P_0 = \text{diag}[1, 000\ 10]$.

The waveform $s_1[n]$ was chosen to be a linear frequency modulated (LFM) chirp of duration 1.5 μs and a frequency sweep of 100 MHz. We used $L = 10$ pulses in each sub-dwell, a pulse repetition interval (PRI) of 100 μs, and a tracker update interval of $\Delta T = 1$ s. The amplitude of the target return was sampled from a zero-mean, complex Gaussian process with covariance matrix $\sigma^2 \mathbb{I}_L$, where σ^2 was chosen to satisfy specified values of SCR. We define the SCR to be the ratio of the target signal power to the *total* power of the clutter in the range bin containing the target. As a measure of the algorithm's performance, we present averaged position RMSE plots conditioned on convergence, where a run was said to have converged if the true target was always located within the validation gate [16]. The plots are compared with the corresponding performance obtained when the fixed LFM chirp waveform alone is transmitted in each dwell, thus representing a non-adaptive system.

In Fig. 2, we compare the magnitude of a typical phase-modulated waveform, designed as described in Section III with that of the LFM chirp transmitted in Sub-dwell 1. The range bins in which the clutter was estimated to be strong, or the elements of the set Z_τ in (6), are marked by asterisks. It can be observed that in these range bins, the magnitude autocorrelation function is upto 30 dB below the corresponding level for the LFM chirp.

Fig. 3 shows a comparison of the averaged position RMSE obtained at the end of Sub-dwells 1 and 2, corresponding to the transmission of the fixed LFM chirp, and the dynamically designed waveform. We observe that the RMSE is lower when the dynamically designed waveform is used thus indicating a performance improvement of more than 20 dB SCR for the same RMSE.

VI. Conclusions

In this paper we presented a waveform-adaptive tracking algorithm that reduces tracking error by improving the detection performance. Using a two-step approach, we first estimate the clutter statistics within the validation gate and then use these estimates to design a phase-modulated waveform for the next transmission. The second waveform helps to improve the SCR in the target location and thus improve detection performance. Since a reduction in the number of false alarms directly reduces uncertainty in the origin of the measurement, the tracking performance improves considerably, as demonstrated in a simulation study. Note that tracking performance can be further improved by adapting the waveform to the dynamic demands of the tracker in addition to the estimates of the environment. This would permit tradeoffs in the delay and Doppler resolution properties of each waveform in addition to their ability to mitigate sea clutter.

Acknowledgements

This work was partly supported by the DARPA *Waveforms for Active Sensing* Program under NRL grant N00173-06-1-G006.

References

[1] D. J. Kershaw and R. J. Evans, "Optimal waveform selection for tracking systems," *IEEE Transactions on Information Theory*, vol. 40, no. 5, pp. 1536–1550, Sep. 1994.

[2] S. D. Howard, S. Suvorova, and W. Moran, "Waveform libraries for radar tracking applications," *International Conference on Waveform Diversity and Design*, Nov. 2004.

[3] S. P. Sira, A. Papandreou-Suppappola, and D. Morrell, "Dynamic configuration of time-varying waveforms for agile sensing and tracking in clutter," *IEEE Transactions on Signal Processing*, 2007, In print.

[4] K. T. Wong, "Adaptive pulse-diverse radar/sonar waveform design," in *IEEE Radar Conference*, May 1998, pp. 105–110.

[5] B. F. L. Scala, W. Moran, and R. J. Evans, "Optimal adaptive waveform selection for target detection," in *International Conference on Radar*, 2003, pp. 492–496.

[6] S. P. Sira, A. Papandreou-Suppappola, D. Morrell, D. Cochran, W. Moran, S. Howard, and R. Calderbank, "Adaptive waveform design for improved detection of low-RCS targets in heavy sea clutter," *IEEE Journal on Special Topics in Signal Processing: Special Issue on Adaptive Waveform Design for Agile Sensing and Communication*, Jun. 2007.

[7] S. M. Sowelam and A. H. Tewfik, "Waveform selection in radar target classification," *IEEE Transactions on Information Theory*, vol. 46, pp. 1014–1029, May 2000.

[8] D. Garren, M. Osborn, A. Odom, J. Goldstein, S. Pillai, and J. Guerci, "Enhanced target detection and identification via optimised radar transmission pulse shape," *IEE Proceedings-Radar Sonar and Navigation*, vol. 148, no. 3, pp. 130–138, 2001.

[9] S. P. Sira, A. Papandreou-Suppappola, and D. Morrell, "Characterization of waveform performance in clutter for dynamically configured sensor systems," *Waveform Diversity and Design Conference*, Jan. 2006, Lihue, Hawaii.

[10] H. L. Van Trees, *Detection Estimation and Modulation Theory, Part III*. New York: Wiley, 1971.

[11] D. J. Kershaw and R. J. Evans, "Waveform selective probabilistic data association," *IEEE Transactions on Aerospace and Electronic Systems*, vol. 33, pp. 1180–1188, Oct. 1997.

[12] D. F. DeLong and E. M. Hofstetter, "On the design of optimum radar waveforms for clutter rejection," *IEEE Transactions on Information Theory*, vol. IT-13, no. 3, pp. 454–463, Jul. 1967.

[13] K. Ward, C. Baker, and S. Watts, "Maritime surveillance radar Part I : Radar scattering from the ocean surface," *IEE Proceedings F: Communications, Radar and Signal Processing*, vol. 137, no. 2, pp. 51–62, Apr. 1990.

[14] S. Haykin, R. Bakker, and B. W. Currie, "Uncovering nonlinear dynamics - The case study of sea clutter," *Proceedings of the IEEE*, vol. 90, pp. 860–881, May 2002.

[15] K. J. Sangston and K. R. Gerlach, "Coherent detection of radar targets in a non-Gaussian background," *IEEE Transactions on Aerospace and Electronic Systems*, vol. 30, no. 2, pp. 330–340, Apr. 1994.

[16] Y. Bar-Shalom and T. E. Fortmann, *Tracking and Data Association*. Boston: Academic Press, 1988.

[17] A. Farina, F. Gini, M. V. Greco, and L. Verrazzani, "High resolution sea clutter data: statistical analysis of recorded live data," *IEE Proceedings on Radar, Sonar and Navigation*, vol. 144, no. 3, pp. 121–130, Jun. 1997.

[18] M. I. Skolnik, *Introduction to Radar Systems*, 3rd ed. McGraw Hill, 2001.

[19] M. Feder and E. Weinstein, "Parameter estimation of superimposed signals using the EM algorithm," *IEEE Transactions on Acoustics, Speech, and Signal Processing*, vol. 36, no. 4, pp. 477–489, Apr. 1988.

[20] J. D. Wolf, G. M. Lee, and C. E. Suyo, "Radar waveform synthesis by mean-square optimization techniques," *IEEE Journal of Oceanic Engineering*, vol. AES-5, no. 4, pp. 611–619, Jul. 1969.

[21] M. S. Arulampalam, S. Maskell, N. Gordon, and T. Clapp, "A tutorial on particle filters for online nonlinear/non-Gaussian Bayesian tracking," *IEEE Transactions on Signal Processing*, vol. 50, pp. 174–188, Feb. 2002.